Energy & Environmental Science

Accepted Manuscript

ROYAL SOCIETY OF CHEMISTRY

www.rsc.org/ees

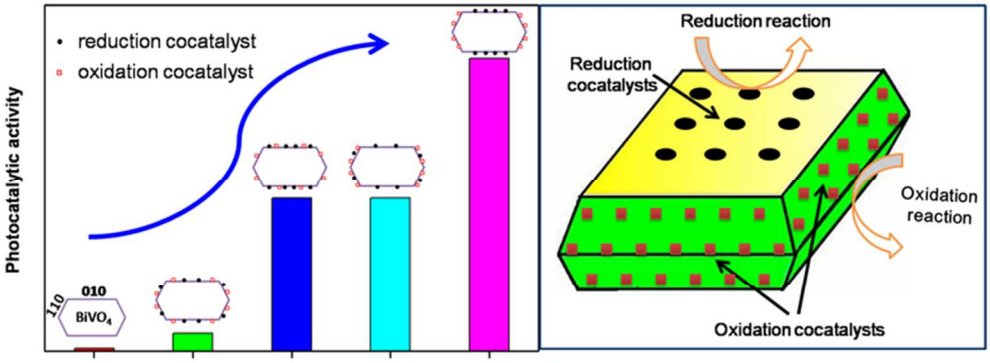

Rational construction of dual cocatalysts corresponding on different facets can efficiently improve the photocatalytic performance.
33x14mm (600 x 600 DPI)

Highly efficient photocatalysts constructed by rational assembly of dual-cocatalysts separately on different facets of $BiVO_4$

Rengui Li[1,2], Hongxian Han[1], Fuxiang Zhang[1], Donge Wang[1] and Can Li[1]*

1. *State Key Laboratory of Catalysis, Dalian National Laboratory for Clean Energy, Dalian Institute of Chemical Physics, Chinese Academy of Sciences, Zhongshan Road 457, Dalian, 116023, China.*
2. *University of Chinese Academy of Sciences, Beijing, 100049, China.*

Abstract.

Cocatalysts play important roles in promoting the catalytic reactions of semiconductor photocatalysts. Especially, deposition of dual cocatalysts, i.e., oxidation and reduction cocatalysts, onto a semiconductor photocatalyst can significantly improve its photocatalytic activity due to synergetic effect of rapid consumption of photogenerated electrons and holes. However, in most cases, the cocatalysts are randomly deposited onto the semiconductor photocatalysts, where the cocatalysts cannot play their full functions. Herein, Based on the findings that photogenerated electrons and holes can be spatially separated onto the different facets of $BiVO_4$, we have successfully prepared two types of photocatalysts ($M/MnO_x/BiVO_4$ and $M/Co_3O_4/BiVO_4$, where M stands for noble metals) with reduction and oxidation cocatalysts selectively deposited onto the {010} and {110} facets of $BiVO_4$ by photo-deposition method. Remarkably enhanced photocatalytic activities were observed for such assembled photocatalysts in control experiments of photocatalytic water oxidation and photocatalytic degradation of methyl orange and rhodamine B. In-depth investigations show that the enhanced photocatalytic performances are due to not only the intrinsic nature of charge separation between the {010} and {110} facets of $BiVO_4$, but also the synergetic effect of dual-cocatalysts deposited onto the different facets of $BiVO_4$. This work further proves the feasibility of the general concepts for approaching efficient artificial photosynthesis systems, namely, engineering of crystal-based photocatalysts by selective deposition of proper reduction and oxidation cocatalysts onto the different

facets of light absorbing semiconductor crystals.

Keywords： photocatalysis; cocatalyst; synergistic effect; crystal facets.

Photocatalytic and photoelectrochemical solar energy conversions are regarded as one of the most promising solutions to address the environmental crisis and energy shortage issues by replacing fossil fuels. [1-4]Suitable cocatalysts for promoting the catalytic reactions are a prerequisite for high photocatalytic performance. [5]In general, noble metals (such as Pt, Pd, Au, Ag etc.) are used as the efficient proton reduction cocatalysts, while some metal oxides (such as IrO_2, RuO_2, CoO_x, MnO_x etc.) analogue to PSII catalyst can serve as the water oxidation cocatalysts for assembling of semiconductor based photocatalysts.[4-9] In most cases, cocatalysts (especially oxidation cocatalysts) were deposited by impregnation or adsorption method, which resulted in a random distribution of cocatalysts on photocatalyst surface without control of the location of cocatalysts. Recently, it was found that photogenerated electron and hole can be spatially separated onto different facets of semiconductors.[10-12] It was also reported that using single-particle fluorescence spectroscopy can be used to demonstrate the reduction and oxidation facets for semiconductors.[13-15] Previously we have found the charge separation between different facet of $BiVO_4$ crystal.[16] So we can assemble proper cocatalysts on different facets of semiconductor based on the charge separation between different facets. To extend this dual cocatalysts selective deposition strategy to develop more efficient photocatalysts, it is necessary to further investigate the universality of this approach by applying other cocatalysts, and verify the function of cocatalysts deposited onto the right facets of semiconductor, namely the reduction cocatalyst on the electron-rich facet and oxidation cocatalyst on the hole-rich facet. It is also attractive to know how

much difference between the photocatalyst systems with selective deposition of cocatalysts on corresponding sites and the randomly distributed cocatalysts.

In this work, we investigated on the relations between the locations of the different cocatalysts on different facets of $BiVO_4$ crystals and the catalytic activities of photocatalysts by tailoring the deposition methods (as shown in scheme 1). Two types of $BiVO_4$ based photocatalysts ($M/MnO_x/BiVO_4$ and $M/Co_3O_4/BiVO_4$, where M stands for noble metals) were rationally designed and prepared. Two kinds of typical photocatalytic reactions, i.e., photocatalytic water oxidation and photocatalytic degradation of methyl orange (MO) and rhodamine B (RhB), were applied for examining the photocatalytic activities of the synthesized photocatalysts. In both cases, the photocatalytic activities of $BiVO_4$ photocatalysts with reduction and oxidation cocatalysts selectively deposited on {010} and {110} facets are dramatically enhanced compared to those of the photocatalysts with the cocatalysts randomly distributed. Systemic studies show that the enhancement of the photocatalytic activity can be attributed to the intrinsic nature of charge separation between the different facets of $BiVO_4$, together with the synergetic effect of co-loaded reduction and oxidation cocatalysts on $BiVO_4$.

Cobalt oxides[17-20] and manganese oxides, [21, 22] which have been reported to be efficient cocatalysts for photocatalytic or photoelectrochemical water oxidation, were deposited as oxidation cocatalysts on hole-rich facets by photo-oxidation deposition method with IO_3^- as an electron acceptor. In the similar way, MnO_x can be also selectively deposited on specific facets of $BiVO_4$.[16] The confirmation of different

facets of as-prepared $BiVO_4$ crystal was introduced according to the previous work.[23] Traditionally, the main exposed facets of $BiVO_4$ is composed of two kinds of facets denoted as {010} and {110} facets, respectively (Figure S1). Figure 1 show the morphology of cobalt cocatalysts deposited $BiVO_4$. It can be clearly seen that small cobalt oxide particles were deposited selectively on the {110} facets of $BiVO_4$. The deposited cobalt oxides were also confirmed by high-resolution TEM (Figure 1c and 1d), in which the planar spaces of 0.202 nm, 0.286 nm and 0.242 nm well match with the standard plane of Co_3O_4[17, 19]. The reduction cocatalyst Pt can be deposited on the electron-rich {010} facets of $BiVO_4$ by photo-reduction deposition method, as visualized by the sharp contrast spots of the Pt nanoparticles in the corresponding SEM image (shown in Figure 1e). It can be seen that the oxidation cocatalysts or reduction cocatalysts can be deposited on the {110} and {010} facets respectively.

Dual cocatalysts, namely the reduction and oxidation cocatalysts, were also selectively deposited on the {010} and {110} facets of $BiVO_4$ by sequential photo-deposition method. As a comparison, $BiVO_4$ samples with randomly distributed dual-cocatalysts were also prepared by impregnation method. Figure 2 shows the SEM images of $Pt/MnO_x/BiVO_4$ and $Pt/Co_3O_4/BiVO_4$ with dual-cocatalysts selectively located on different facets and randomly distributed on all facets. From figure 2a and 2c (2b and 2d), we can clearly see the different location of dual-cocatalysts on these photocatalysts: the dual-cocatalysts were separately deposited on {010} and {110} facets of $BiVO_4$ (2a and 2b) with the photo-deposition method, or deposited on all facets (2c and 2d) with the impregnation method.

Selective deposition of dual cocatalysts by photo-deposition method and randomly deposition of dual cocatalysts by impregnation method can be more clearly visualized on the SEM images of $BiVO_4$ with larger amounts of cocatalysts (2 wt %) deposited (Figure S2 and S3). Although the particle sizes (especially for Pt) are slightly different with different deposition methods, the exposed active surface of cocatalysts by CO adsorption experiment are comparable (Table S1). To further confirm the assignment of different cocatalysts on different facets, the SEM images of the deposition of single cocatalysts by photo-deposition and impregnation method were also showed respectively (FigureS4 and Figure S5). Compared with each other, we can get a clear description about selectively distribution and randomly distribution of cocatalysts to confirm the assignment of different cocatalysts on different facets. EDX analysis for different ranges of $BiVO_4$ crystal also shows that different particles on different facets represent for MnO_x (Co_3O_4) and Pt respectively (Figure S6). Controllable deposition of dual cocatalysts by different deposition method facilitates us for more in-depth investigation of the effect of the cocatalyst location facets.

To rule out the possibility of formation of different cocatalyst species by different deposition methods, the cobalt and manganese oxides deposited with different methods were further investigated by XPS characterization (Figure S7a). Almost identical binding energy of 777.9 and 795.0 eV were observed for both samples though cobalt oxide were deposited by different methods, demonstrating that the same Co_3O_4 species were formed in both cases, which are consistent with the HRTEM observation shown in Figure 1. Similar result was also obtained for MnO_x deposited

by photo-deposition or impregnation method (Figure S7b). It should be pointed that the cocatalyst species can be reduced or oxidized by the photoexited electrons and holes from photocatalyst during the photocatalytic reaction because the electrons and holes were trapped by cocatalysts first and then for the following redox reaction.[24] It means that the cocatalyst can be reduced or oxidized to the most stable and suitable state in this process. In our experiment, XPS characterization was used to make sure there are almost no differences between different cocatalysts deposited by different method before the photocatalytic reaction. We also characterized them after the photocatalytic reaction and they showed the similar results (not shown).These XPS analysis results indicate that the different photocataltyic performances between the photocatalysts with cocatalysts deposited by different method are not due to cocatalyst species.

In order to evaluate the photocatalytic performance for the photocatalysts with selectively and randomly distributed dual-cocatalysts, two typical reactions were conducted: photocatalytic water oxidation reaction, and photocatalytic degradation (oxidation) of dye molecules. To make the photocatalytic performances comparable, equal amounts of the cocatalysts were deposited with the different deposition methods.

Photocatalytic water oxidation for the powder photocatalyst was evaluated using IO_3^- as electron acceptor in a closed gas circulation system. The whole process involves two reactions, one is the reduction of IO_3^- and the other is the oxidation of water (equations 1 and 2). It is a thermodynamically unfavorable reaction and the

exited photons from photocatalysts should supply energy to overcome it (Scheme S1). The reduction cocatalyst and oxidation cocatalyst deposited on $BiVO_4$ act as the reaction sites for both reduction and oxidation reactions respectively.

$$2H_2O + 4h^+ \rightarrow O_2 + 4H^+ \quad (1)$$

$$4H^+ + \frac{2}{3}IO_3^- + 4e^- \rightarrow \frac{2}{3}I^- + 2H_2O \quad (2)$$

Table 1 gives the photocatalytic water oxidation performance of $Pt/Co_3O_4/BiVO_4$ system with dual-cocatalysts located on different facets. To clearly illustrate the effect of cocatalyst locations on photocatalytic water oxidation activities, the scheme of cocatalysts location facets is also shown at the top of the Table. The deposition of reduction and (or) oxidation cocatalysts can trap electrons and (or) holes for surface catalytic reactions, so that to improve the charge separation efficiency. For example, when Pt was deposited on $BiVO_4$, the Schottky barrier is formed at the interface to facilitate the charge separation, which facilitates separation of photogenerated charges by transferring electrons to Pt.[5, 25] However, the catalytic function of cocatalysts can be fully fulfilled only when they are located on the right active sites. Compared with entry 2 and 3, we can see that the selective deposition of Pt shows better performance than that with randomly deposited cocatalysts. In addition, the surface area of {010} and {110} facets were estimated to be almost the same for as-prepared $BiVO_4$. Nevertheless, 100 % of the Pt nanopariticles were exclusively deposited on {010} facets by photo-deposition method while Pt nanoparticles were randomly deposited on both {010} and {110} facets (roughly estimated to be 50 %: 50 % distribution) by the impregnation method. Interestingly, the photocatalytic water oxidation activity of

entry 2 is nearly half of the entry 3 (A2≈½×A3), indicating that only the Pt nanoparticles located on {010} can have positive effect on water oxidation reaction but those Pt nanoparticles deposited on {110} facets do not contribute to the water oxidation activity. Similar trend can also be found for Co_3O_4 cocatalyst by comparison of entry 4 and 5(A4≈½×A5). These results indicate that the cocatalysts can perform the function only when they are located on the right facets. The cocatalysts located on the wrong facets, e.g., oxidation cocatalysts on electron-rich sites or reduction cocatalysts on hole-rich sites, will not do any contribution to the catalytic activities.

Comparison of entries 6 and 7 also shows that the samples with one of the dual-cocatalysts (either Pt or Co_3O_4) selectively deposited on {010} or {110} facets of $BiVO_4$ and another one deposited randomly show much better photocatalytic performances than those of the $BiVO_4$ samples with only one of the reduction or oxidation cocatalysts deposited. Most importantly, the synergetic effect of dual cocatalysts can be found when one of the cocatalysts was located on right facets [(A2+A5) <<A6, (A3+A4) <<A7)]. However, almost no synergetic effect was obtained when dual-cocatalysts were randomly deposited on every facet (A2+A4≈A8). Interestingly, when the reduction and oxidation cocatalysts were selectively deposited on the right facets, the highest photocatalytic activity is achieved (entry 9), which is 17 times of that with dual-cocatalysts located randomly (entry 8). The most remarkable synergetic effects were observed for the Pt and Co_3O_4 selectively deposited on the {010} or {110} facets of $BiVO_4$, respectively, evidenced by the sum

of the photocatalytic activities of entry 3 and 5 are much less than that of entry 9 (A3+A5<<A9). In addition, it can be seen that the photocatalytic activities of entry 6 and entry 7 are close to half of that of entry 9 (A6≈½×A9, A7≈½×A9). This further confirms that no obvious synergetic effect was found when Pt or Co_3O_4 were located on the wrong facets if one considers the probability of cocatalysts deposition on the two different facets would be roughly 50%:50%. These results indicate that the synergetic effect can be found when the either single cocatalyst or dual-cocatalysts are located on the right facets, especially when both of them are located on the right facets, this effect can be fully functioned to reach a higher level.

For water oxidation reaction, when only Pt was deposited as a cocatalyst, the water oxidation activity was increased much more obvious than Co_3O_4 only as the cocatalyst (entries 3 and 5). It seems that the reduction of IO_3^- is possible the rate-determining step of this reaction. However, when only reduction cocatalyst was deposited but without oxidation cocatalyst, the reaction activity is still low enough. For this case, the deposition of oxidation cocatalyst can greatly enhance the whole reaction activity (A6=10A2, A9=10A3). It indicates that only when the reduction reaction rate and oxidation reaction rate were accelerated simultaneously can we get the much higher reaction rate than any other one, namely, the synergistic relationship of the reduction and oxidation reaction can be fully functioned in this case.

Photoelectrochemical water oxidation performance of $BiVO_4$ with cobalt oxides deposited on different facets was also examined to further demonstrate the importance of rational distribution of cocatalyst on right facets. In this case, Pt was used as a

counter electrode. It can regarded as a resemble of reduction cocatalyst deposited on powder photocatalyst since electrons can be driven to Pt under the bias (Figure S8). When the Co_3O_4 cocatalyst was selectively deposited on {110} facets, the photocurrent was increased to 5 times of the $BiVO_4$ electrode with the oxidation cocatalyst Co_3O_4 randomly deposited on both {010} and {110} facets. This indicates that the photocurrent can be efficiently promoted when the oxidation cocatalyst (trapping holes) is selectively deposited on the {110} facets, which is in well agreement with the results of the photocatalytic water oxidation experiments.

To further confirm the predominant catalytic effect of selective distribution of dual-cocatalysts on different facets, photocatalytic degradation (oxidation) of environmental pollutants is also investigated. We chose methyl orange (MO) and rhodamine B (RhB) as model pollutant molecules to evaluate the photocatalytic performance of $BiVO_4$ with cocatalyts rationally located on different facets. The reaction processes can be summarized similarly as reported (Scheme S2).[26-28].

Table 2 shows the photocatalytic performances of degradation of pollutants (MO and RhB). Overall, similar catalytic activity trends as water oxidation were obtained for both degradation of MO and RhB. It can be seen that loading with the single reduction or oxidation cocatalyst can only achieve low activities for degradation of both MO and RhB. Meanwhile, relatively low degradation performances were obtained for all photocatalysts which have the reduction and/or oxidation cocatalysts randomly deposited by impregnation method. These results indicate that merely reduction or oxidation cocatalyst loaded, or randomly distribution of dual cocataysts

on $BiVO_4$ can only lead to relatively low photocatalytic activities due to inefficient charge utilization. However, much better performances can be achieved for Pt (P.D.)/ MnO_x(P.D.) /$BiVO_4$ samples which has Pt and MnO_x selectively deposited on {010} and {110} facets respectively. Compared with the $BiVO_4$ sample with dual-cocatalysts randomly distributed, it shows 9 times higher activity for degradation of RhB and 7 times higher activity for degradation of MO. The remarkable synergetic effect of dual cocatalysts is also evident by comparison of $BiVO_4$ with single cocatalyst selectively deposited on the right facets and with dual cocatalysts selectively deposited on the corresponding right facets ($k3+k5 \ll k8$). However, no synergetic effect was observed for Pt/Co_3O_4/$BiVO_4$ system, which may be due to the mismatch of energy structures between Co_3O_4 and dye molecules. In addition, the time curves for photocatalytic degradation of MO and RhB were also shown (Figure S9). The experiments on photocatalytic degradation of dyes further confirms that the remarkably enhanced photocatalytic activity of Pt/MnO_x/$BiVO_4$, which has Pt and MnO_x selectively deposited on the electron-rich {010} facet and hole-rich {110} facet, is mainly due to the synergetic effect of dual-cocatalysts, though the intrinsic charge separation between the different facets upon photoexcitation cannot be ignored. Probably, these two effects may be synchronized in real photocatalytic processes with the dual cocatalyts play significant roles in further spatial charge separation and providing active catalytic sites, leading to dramatically enhanced photocatalytic activity.

Above two typical reactions (photocatalytic water oxidation, photocatalytic

degradation of methyl orange and rhodamine B) consistently show that the rational loading of reduction and oxidation cocatalysts selectively on different facets of $BiVO_4$ can significently enhance the photocatalytic activity. The super performances were mainly attributed to the efficient charge separation between different facets and the synergetic effect of dual-cocatalysts. Since electrons and holes enriches respectively on {010} and {110} facets of $BiVO_4$ upon photoexcitation, reduction and oxidation cocatalysts can be selectively deposited onto these facets by photo-deposition method. During photocatalytic reaction processes, the photogenerated electrons and holes might be excited onto the {010} and {110} facets, respectively, generating transient electron-rich {010} facets and hole-rich {110} facets. Due to reduction and oxidation cocatalysts are deposited onto the {010} and {110} facets, respectively, the photogenerated electrons and holes can be further transferred to these cocatalysts for the surface catalytic reactions. Photocatalytic water oxidation and degradation of dyes are all mainly oxidation reactions. However, all of the oxidation reactions simultaneously involve reduction reactions. In order to obtain highly efficient photocatalytic activity, one must consider not only the oxidation reactions of photogenerated holes, but also the reduction reactions of photogenerated electrons. In other words, in order to assembly efficient photocatalysts, whether the desired reaction is oxidation reaction or reduction reaction, one must simultaneously deal well with both oxidation and reduction reactions using proper cocatalysts. And this is the reason why the functionality of dual cocatalysts can be fully fulfilled only when they are located on the right active sites.

The choice of proper reduction and oxidation cocatalysts is another important factor for constructing such kind of selectively deposited dual cocatalysts system. To demonstrate the general functional scenario of dual cocatalyts strategy, we further extended the cocatalyts to some other metals and oxides. Similarly, these photocatalysts were also subject to investigation on photocatalytic water oxidation activities in different combinations of cocatalysts deposited on different facets of $BiVO_4$.

Different oxidation cocatalysts were tested while Pt as the reduction cocatalyst. As some metal oxides cocatalysts are difficult to be deposited by photo-deposition method, the selected metal oxides (NiO, CuO, and Fe_2O_3) were deposited by impregnation method. It should be pointed out that nearly no photocatalytic water oxidation activity when only these metal oxides were deposited using IO_3^- as electron acceptors. Figure 3a shows that all the photocatalysts with dual-cocatalysts reveal higher activity than that of Pt/$BiVO_4$, especially when Co_3O_4 and Fe_2O_3 are used as the oxidation cocatalysts, suggesting that there is remarkable synergetic effect of the dual-cocatalysts. The different photocatalytic performances by deposition of different cocatalysts may be ascribed to the different matching degree of energy band level structures between metal oxides and $BiVO_4$.

Correspondingly, different reduction cocatalysts were also employed with MnO_x and Co_3O_4 as fixed oxidation cocatalysts. Figure 3b shows the photocatalytic performance of different reduction cocatalyst (Ag, Au and Pt) with MnO_x or Co_3O_4 acting as oxidation cocatalyst. The much better performances (more than 10 times)

were obtained for different dual-cocatalysts loaded $BiVO_4$ than $MnO_x/BiVO_4$ or $Co_3O_4/BiVO_4$. The same trends were observed for both systems with MnO_x and Co_3O_4 acting as oxidation cocatalysts. The activity order is Pt>Au>Ag, which is possibly due to the different work functions of noble metals (Pt, 5.03; Au, 4.78; Ag, 4.30). It indicates that different kinds of reduction cocatalysts showed different photocatalytic performance and the better charge separation and utilization efficiency could be obtained even when different reduction cocatalysts were employed. All these results of different combinations of dual-cocatalysts by changing different reduction cocatalysts or oxidation cocatalysts revealed the generality and superiority of rationally constructing selectively deposited dual-cocatalysts photocatalytic systems.

In summary, we rationally designed and prepared a series of $BiVO_4$-based photocatalysts by selective deposition of reduction and oxidation cocatalysts on the {010} and {110} facets of $BiVO_4$, respectively. Two photocatalyst systems ($M/MnO_x/BiVO_4$ and $M/Co_3O_4/BiVO_4$, M stands for noble metals) were invesigated for two types of photocatalytic reactions (photocatalytic water oxidation, and photocatalytic degradation of methyl orange and rhodamine B) to demonstrate the strategy. Remarkably enhanced photocatalytic activities were observed for such assembled photocatalysts. In-depth investigations show that the enhanced photocatalytic performances are due to not only the intrinsic nature of charge separation between the {010} and {110} facets of $BiVO_4$, but also the synergetic effect of dual-cocatalysts deposited on different facets of $BiVO_4$. This work further proves the feasibility of our general concepts for approaching efficient artificial

photosynthesis systems, namely, engineering of crystal-based photocatalysts by selective deposition of proper reduction and oxidation cocatalysts on different facets of visible light absorbing semiconductor crystals.

Acknowledgements

This work was financially supported by 973 National Basic Research Program of the Ministry of Science and Technology (Grant 2014CB239400); National Natural Science Foundation of China (No. 21061140361, 21090340) and"Hundred Talents Program" of Chinese Academy of Sciences. Rengui Li would like to thank the support from Haldor-Topsoe Company of Denmark.

References.

1 A. Fujishima and K. Honda, *Nature* 1972, **238**, 37-38.

2 K. Maeda, K. Teramura, D. L. Lu, T. Takata, N. Saito, Y. Inoue and K. Domen, *Nature* 2006, **440**, 295-295.

3 S. Y. Reece, J. A. Hamel, K. Sung, T. D. Jarvi, A. J. Esswein, J. J. H. Pijpers and D. G. Nocera, *Science* 2011, **334**, 645-648.

4 A. Kudo and Y. Miseki, *Chem. Soc. Rev.* 2009, **38**, 253-278.

5 J. H. Yang, D. E. Wang, H. X. Han and C. Li, *Acc. Chem. Res.* 2013, **46(8)**, 1900-1909.

6 M. Ni, M. K. Leung, D. Y. Leung and K. Sumathy, *Renew. Sust. Energ. Rev.* 2007, **11**, 401-425.

7 K. Maeda and K. Domen, *J. Phys. Chem. Lett.* 2010, **1**, 2655-2661.

8 X. B. Chen, S. H. Shen, L. J. Guo and S. S. Mao, *Chem. Rev.* 2010, **110**, 6503-6570.

9 S. S. K. Ma, K. Maeda, R. Abe and K. Domen, *Energy Environ. Sci.* 2012, **5**, 8390-8397.

10 J. Pan, G. Liu, G. Q. M. Lu and H. M. Cheng, *Angew. Chem. Int. Ed.* 2011, **50**, 2133-2137.

11 G. Liu, C. Y. Jimmy, G. Q. M. Lu and H. M. Cheng, *Chem. Commun.* 2011,**47**, 6763-6783.

12 T. Ohno, K. Sarukawa and M. Matsumura, *New J. Chem.* 2002, **26**, 1167-1170.

13 T. Tachikawa and T. Majima, *Chem. Soc. Rev.* 2010, **39**, 4802-4819.

14 T. Tachikawa, S. Yamashita and T. Majima, *J. Am. Chem. Soc.* 2011, **133**, 7197-7204.

15 T. Tachikawa, N. Wang, S. Yamashita, S. C. Cui and T. Majima, *Angew. Chem. Int. Ed.* 2010, **49**, 8593-8597.

16 R. G. Li, F. X. Zhang, D. E. Wang, J. X. Yang, M. R. Li, J. Zhu, X. Zhou, H. X. Han and C. Li, *Nat. Commun.* 2013, **4**, 1432. DOI: 10.1038/ncomms2401.

17 F. X. Zhang, A. Yamakata, K. Maeda, Y. Moriya, T. Takata, J. Kubota, K. Teshima, S. Oishi and K. Domen, *J. Am. Chem. Soc.* 2012, **134**, 8348-8351.

18 M. J. Liao, J. Y. Feng, W. J. Luo, Z. Q. Wang, J. Y. Zhang, Z. S. Li, T. Yu and Z. G. Zou, *Adv. Func. Mater.* 2012, **22**, 3066-3074.

19 R. G. Li, Z. Chen, W. Zhao, F. X. Zhang, K. Maeda, B. K. Huang, S. Shen, K. Domen and C. Li, *J. Phys. Chem. C* 2012, **117**, 376-382.

20 Y. Q. Cong, H. S. Park, S. J. Wang, H. X. Dang, F. R. F. Fan, C. B. Mullins, A. J. Bard, *J. Phys. Chem. C* 2012, **116**, 14541-14550.

21 K. Maeda, A. K. Xiong, T. Yoshinaga, T. Ikeda, N. Sakamoto, T. Hisatomi, M. Takashima, D. L. Lu, M. Kanehara, T. Setoyama T. Teranishi and K. Domen, *Angew. Chem. Int. Ed.* 2010, **122**, 4190-4193.

22 N. Nishimura, J. Tanikawa, M. Fujii, T. Kawahara, J. Ino, T. Akita, T. Fujino and H. Tada, *Chem. Commun.* 2008, 3564-3566.

23 D. E. Wang, H. F. Jiang, X. Zong, Q. Xu, Y. Ma, G. L. Li and C. Li, *Chem-A Eur. J.* 2011, **17**, 1275-1282.

24 N. L. Wu and M. S. Lee, *Inter. J. Hydro. Energy* 2004, **29**, 1601-1605.

25 D. Y. Leung, X. L. Fu, C. F. Wang, M. Ni, M. K. Leung, X. X. Wang and X. Z. Fu, *ChemSusChem* 2010, **3**, 681-694.

26 D. S. Bhatkhande, V. G. Pangarkar and A. A. Beenackers, *J. Chem. Technol. Biotechnol.* 2002, **77**, 102-116.

27 J. C. Zhao, C. C. Chen and W. H. Ma, *Top. Catal.* 2005, **35**, 269-278.

28 I. K. Konstantinou and T. A. Albanis, *Appl. Catalysis B: Environ.* 2004, **49**, 1-14.

Figures and options.

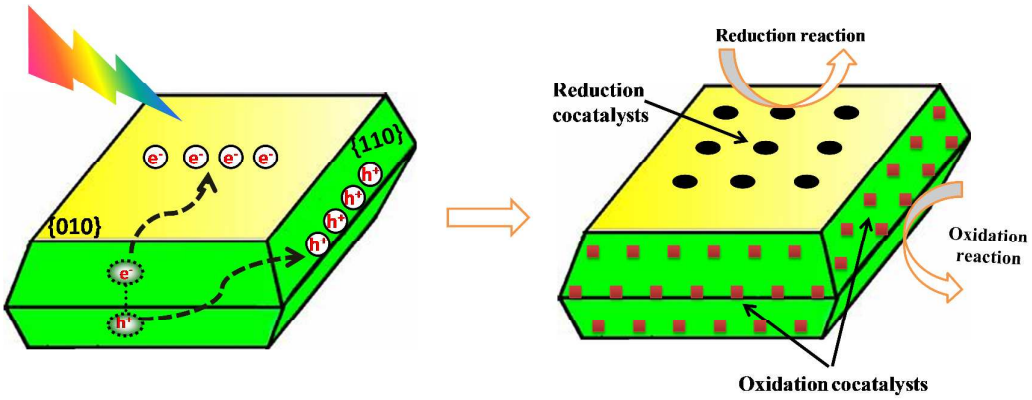

Scheme 1. The scheme of selective deposition of reduction and oxidation cocatalysts on {010} and {110} facets of $BiVO_4$ based on the charge separation between different facets.

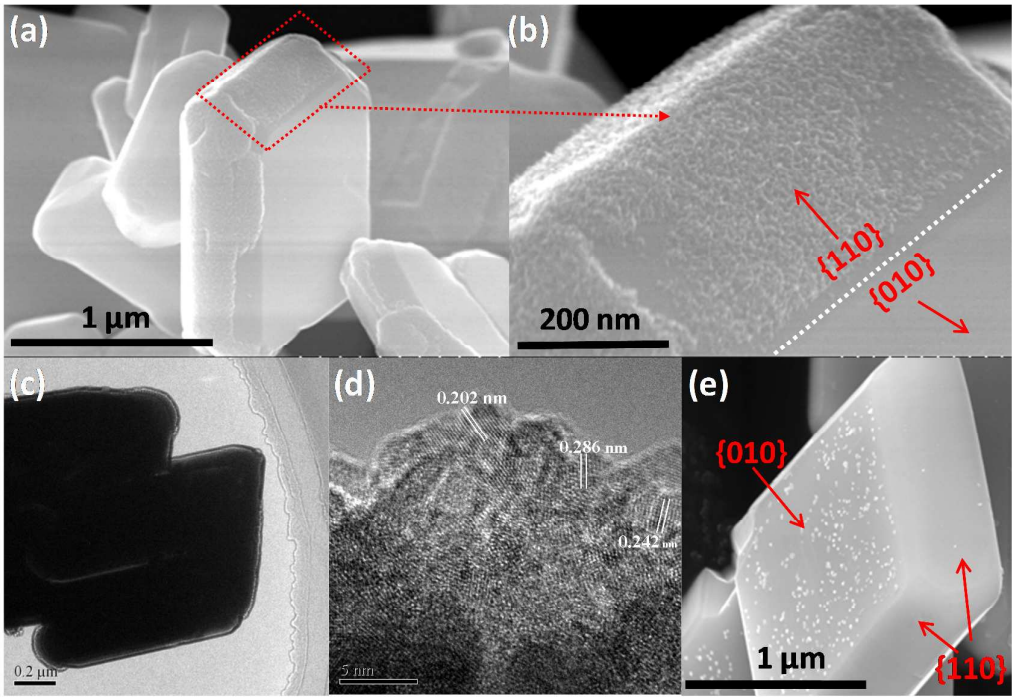

Figure 1.SEM images of CoO_x deposited on {110} facets of $BiVO_4$ by photo-oxidation deposition (a, b); high-resolution TEM images of $CoO_x/BiVO_4$ (c, d); SEM image of Pt as reduction cocatalyst deposited on {010} facets of $BiVO_4$ (e). The contents of the deposited CoO_x and Pt are 2wt %.

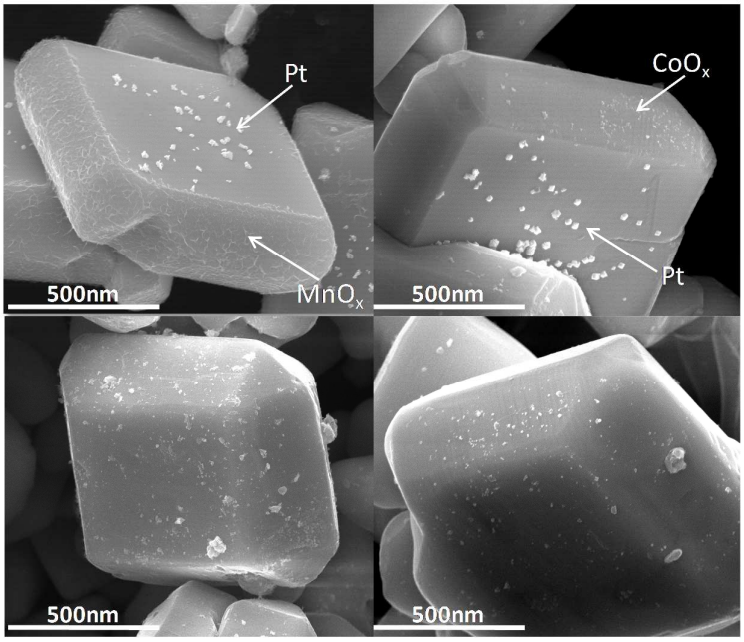

Figure 2.SEM images of $Pt/MnO_x/BiVO_4$ and $Pt/Co_3O_4/BiVO_4$ dual-cocatalysts system prepared by photo-deposition and impregnation method. (a) Pt(P.D.)/ MnO_x(P.D.)/$BiVO_4$; (b) Pt(P.D.)/Co_3O_4(P.D.)/$BiVO_4$ (c) Pt(imp)/MnO_x(imp)/ $BiVO_4$ and (d) Pt(imp)/Co_3O_4(imp)/$BiVO_4$.

Table 1.Photocatalytic water oxidation performances of $BiVO_4$ with cocatalytsts deposited by different methods.

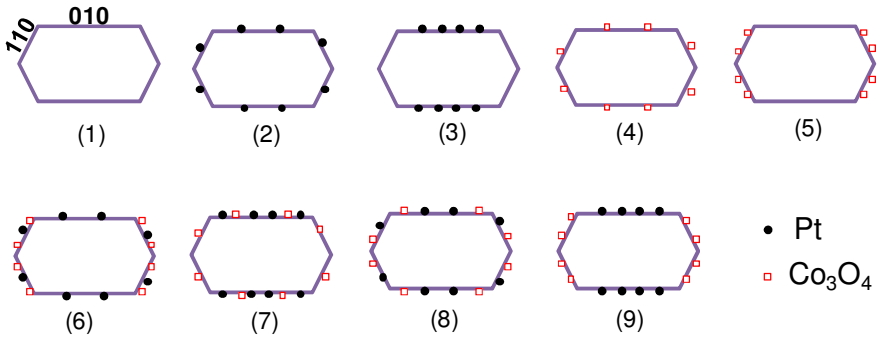

Entry	Pt cocatalysts	Co_3O_4 cocatalysts	The amount of O_2 evolution (μmol/h)
1	--	--	1.0
2	imp[a]	--	8.7
3	P.D. [b]	--	16.1
4	--	imp	1.8
5	--	P.D.	2.5
6	imp	P.D.	87.0
7	P.D.	imp	84.2
8	imp	imp	9.6
9	P.D.	P.D.	160.3

[a] Impregnation method, [b] photo-deposition method. Reaction conditions: 0.15 g Cat., 150mL 0.02 M $NaIO_3$ aqueous solution, 300 W Xe lamp ($\lambda \geq 420$ nm), top irradiation, reaction time:1 h. The contents of the deposited Pt and Co_3O_4 are optimized to be 0.5 wt% and 0.075 wt% respectively.

Table 2.Photocatalytic degradation of methyl orange and rhodamine B on $BiVO_4$ with cocatalysts deposited by different methods.

Entry	Photocatalysts	$k^{[a]}$ (RhB) ($*10^{-3}min^{-1}$)	$k^{[a]}$ (MO) ($*10^{-3}min^{-1}$)
1	blank	0.67	0.8
2	$BiVO_4$	1.7	1.4
3	Pt(P.D.)/ $BiVO_4$	14.4	8.3
4	Pt(imp)/ $BiVO_4$	6.2	5.4
5	MnO_x(P.D.)/ $BiVO_4$	5.4	3.5
6	MnO_x(imp)/ $BiVO_4$	4.3	2.4
7	Pt(P.D.)/ MnO_x(P.D.)/ $BiVO_4$	63.1	46.2
8	Pt(imp)/ MnO_x(imp)/ $BiVO_4$	7.6	7.4
7	Co_3O_4(P.D.)/ $BiVO_4$	5.0	2.8
8	Co_3O_4(imp)/ $BiVO_4$	4.1	2.4
9	Pt(P.D.)/ Co_3O_4(P.D.)/ $BiVO_4$	17.6	12.4
10	Pt(imp)/ Co_3O_4(imp)/ $BiVO_4$	7.7	7.5

[a]k is the apparent first-order rate constant, form the equation: $kt=-In(C/C_0)$, where C_0 and C are the concentrations of dye in solution at times 0 and t, respectively.

Reaction conditions: 50 mg Cat., 100mL dye solution with concentration of 10 mg/L, O_2 bubble, reaction temperature, 288 K, 300W Xe lamp ($\lambda \geq 420$ nm), top irradiation.

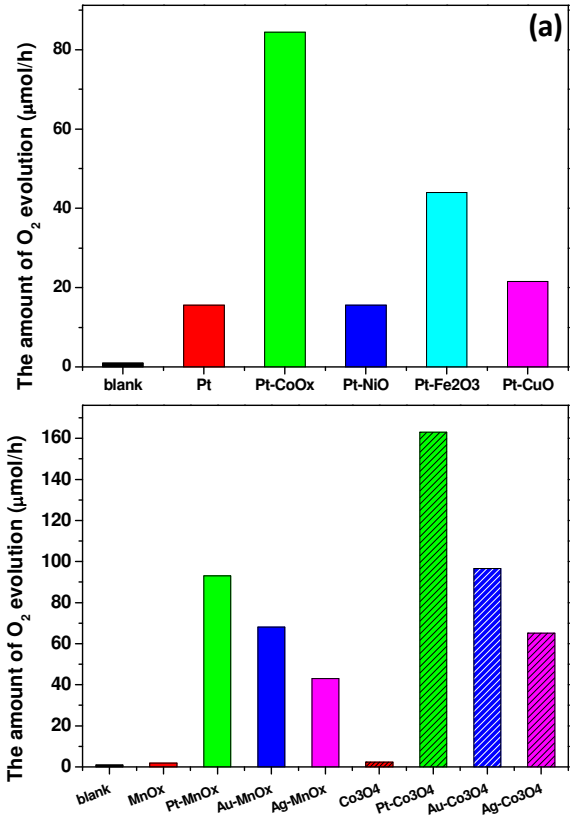

Figure 3. Photocatalytic water oxidation performances of $BiVO_4$ with different combination of reduction and oxidation cocatalysts. (a) Photocatalytic water oxidation activities of $BiVO_4$ with different oxidation cocatalysts when Pt is fixed as the reduction cocatalyst. The reduction cocatalyst was deposited by photo-deposition method and the different oxidation cocatalysts were deposited by impregnation method. (b) Photocatalytic water oxidation activities of different reduction cocatalysts when MnO_x or Co_3O_4 are fixed as the oxidation cocatalysts. The reduction and oxidation cocatalysts were deposited by photo-deposition method. Reaction conditions: In all cases, the amount of cocatalysts was set to be 0.1 wt% in 150 mL 0.02 M $NaIO_3$ aqueous solution, light source: 300 W Xe lamp ($\lambda \geq 420$ nm), top irradiation, reaction time: 1 h.

Table of Content.

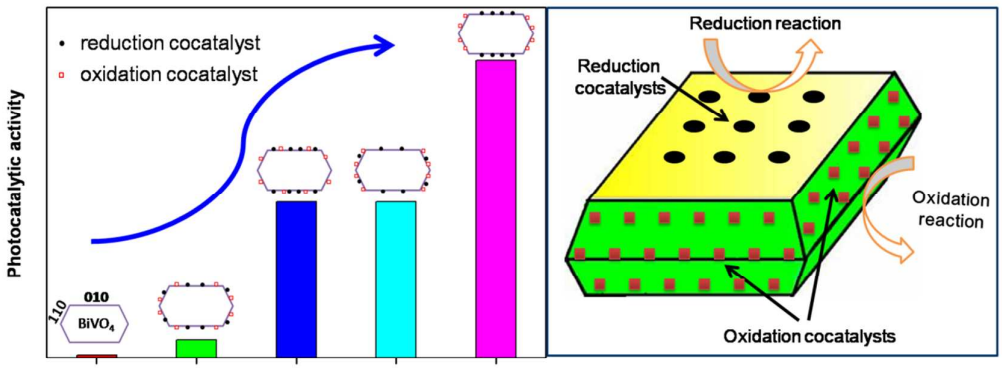

Rational construction of dual cocatalysts corresponding on different facets with photogenerated charge separation.